Carbon-13 Spin–Lattice Relaxation Studies and Their Application to Organic Chemical Problems

George C. Levy

General Electric Corporate Research and Development, Schenectady, New York 12301

Received October 26, 1972

Carbon-13 spin–lattice relaxation studies can give the chemist a new set of parameters that may be used to characterize organic molecular systems. The information derivable from ^{13}C relaxation measurements is generally unobtainable from the more familiar nmr chemical shift, spin–spin coupling, and peak area (integration) parameters. Relaxation data relate closely to overall and local molecular geometry, bonded and nonbonded interactions, and other factors controlling molecular motions. Important applications will be found in studies of molecular structure and stereochemistry, and also in investigations of second-order effects due to solvation and other weak molecular interactions.

Practical and versatile ^{13}C relaxation studies have been closely related to the development and increasing use of pulsed Fourier transform (FT) nmr.[1] In pulsed FT nmr experiments, all ^{13}C nuclei in a sample are excited simultaneously by a short, powerful pulse of radiofrequency energy. Immediately following this excitation the nuclei begin to return to their preexcitation state (by the processes of spin–spin and spin–lattice relaxation). The signal detected in the spectrometer following excitation, called a free induction decay (FID), contains the frequency and intensity information for all the ^{13}C nuclei that were excited. Fourier transformation of the FID in a digital computer reproduces this information as a frequency spectrum equivalent to that obtained from a slow sweep through the entire ^{13}C spectral region.

The advantage of the FT method is that the entire process of excitation and detection of the FID occurs very rapidly (typically in 1 sec). In FT spectrometers pulses are usually applied to the sample repetitively, with coherent addition of the FID's. This form of computer time-averaging is superior to repetitive scanning of the spectrum because of the much shorter time base for each successive spectrum acquisition. In this way natural abundance ^{13}C nmr spectra of 0.2–1 *M* solutions can be routinely obtained on FT spectrometer systems in just a few minutes.

Reported applications of ^{13}C nmr have expanded markedly since commercial FT instrumentation became available in 1970.[2] The application of carbon-13 relaxation measurements to problems of chemical interest has closely followed other ^{13}C developments. Before discussing applications, however, a brief introduction to the phenomenon of spin relaxation is in order.

The Rotating Frame of Reference

The nmr experiment can be considered in a way that simplifies explanations of spin–lattice and spin–spin relaxation: the so-called rotating frame of reference.[3] In the rotating frame, the entire coordinate system rotates at the Larmor, or resonance frequency, corresponding to the experimental laboratory magnetic field, H_0. Figure 1[2] depicts nmr excitation and relaxation in the rotating frame. The characteristic of the nuclear spins (here, ^{13}C nuclei) that is considered in Figure 1 is *M*, the net magnetization of the entire ensemble of nuclear spins. *M* corresponds to the sum of all the individual nuclear magnetic moments.

When a sample is placed in the magnetic field, there is initially no polarization of the nuclear spins. The populations of the two quantized ^{13}C energy levels aligned with and against H_0 are equal and, thus, $M = 0$ (Figure 1a). Interactions between the individual ^{13}C nuclei and their surroundings (the lattice) eventually result in establishment of an equilibrium excess of ^{13}C nuclei in the lower energy level, according to the Boltzmann distribution law. The result is a small equilibrium magnetization, M_0, aligned with the direction of the magnetic field (Figure 1b). The net magnetization remains equal to M_0 only until rf excitation of the sample is initiated.

When the sample is irradiated, the radiofrequency field H_1 at the ^{13}C frequency is applied along the *x* axis, fixed in the rotating frame, as shown in Figures 1c and 1g. The magnetic component of the rf field rotates *M* about the *x* axis, out of alignment with H_0 (the *z* axis) and toward the *y* axis. In pulse nmr this process is very rapid, normally precluding relaxation during the irradiation. The pulse can be applied for an experimentally determined time (usually 1 to 100 μsec) to result in tipping *M* by 90° (Figure 1c) or the pulse width may be twice as long, causing *M* to completely invert (Figure 1g).

Immediately following every excitation pulse the process of spin–lattice relaxation begins. In the con-

George C. Levy attended Syracuse University (A.B., 1965) and then did graduate work, receiving his Ph.D. at the University of California, Los Angeles, in 1968. He is in charge of nmr spectroscopy in the Materials Characterization Operation at the General Electric Research and Development Center, and teaches a graduate level nmr course at Rensselaer Polytechnic Institute. He is author of a recent book on carbon-13 nmr.

(1) (a) R. R. Ernst and W. A. Anderson, *Rev. Sci. Instrum.*, **37**, 93 (1966); (b) T. C. Farrar and E. D. Becker, "Pulse and Fourier Transform NMR," Academic Press, New York, N. Y., 1971; (c) D. A. Netzel, *Appl. Spectrosc.*, **26**, 430 (1972).

(2) G. C. Levy and G. L. Nelson, "Carbon-13 Nuclear Magnetic Resonance for Organic Chemists," Wiley-Interscience, New York, N. Y., 1972.

(3) I. I. Rabi, N. F. Ramsey, and J. Schwinger, *Rev. Mod. Phys.*, **26**, 167 (1954).

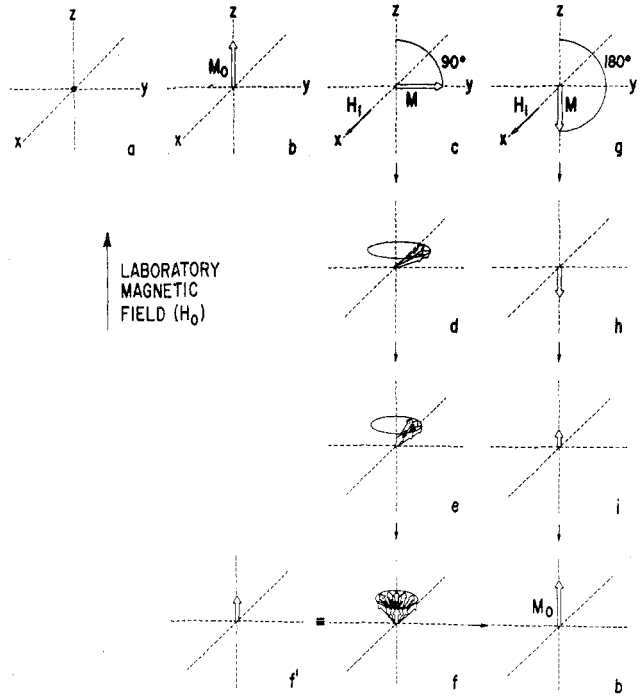

Figure 1. The pulse nmr experiment in the rotating frame.[2] Sequences c–f,b and g–i,b demonstrate relaxation processes.

text of the rotating frame, spin–lattice relaxation is relaxation along the z axis whereas spin–spin relaxation corresponds to relaxation in the x–y plane. The former can be considered as an enthalpy process and the latter an entropy process. Figures 1h and 1i show the return of M to M_0 following a single 180° pulse. In this case only spin–lattice relaxation is visible since there is no net x–y magnetization. M returns to M_0 according to first-order kinetics, with a rate constant $1/T_1$. T_1 is defined as the spin–lattice relaxation time. No free induction decay is observed following an isolated 180° pulse. *The signal detected in nmr spectrometers is the net magnetization in the x–y plane, which is zero in this case.* An isolated 90° pulse, on the other hand, causes M to coincide with the y axis, *in the x–y plane* (Figure 1c). The decay of the x–y magnetization as a function of time forms the free induction decay, discussed above. Following the 90° pulse both spin–lattice and spin–spin relaxation processes begin (Figures 1d to 1f). The x–y magnetization "dephases" as a function of the spin–spin relaxation time T_2 as M simultaneously returns vertically toward M_0 (the T_1 process). No signal is observed after the x–y magnetization is completely dephased, even if z-axis relaxation is incomplete (Figure 1f; this corresponds to T_2 shorter than T_1). The FID normally is a function of T_2^*, not T_2; T_2^* contains contributions to dephasing from magnetic field inhomogeneities and instrumental instabilities.

Spin–Lattice Relaxation Mechanisms

The process of spin–lattice relaxation allows the lattice to act as a *heat sink* for energy absorbed by nuclei when they are irradiated. A mechanism *coupling* the nuclear spins and the lattice is required in order to have efficient energy transfer. All of the mechanisms possible for ^{13}C nuclei share one characteristic: they depend on the presence of fluctuating localized magnetic fields at or near the nucleus being relaxed. The four relaxation mechanisms that are generally considered arise from dipole–dipole interactions, the spin–rotation interaction, chemical shift anisotropy, and scalar interactions. All of these mechanisms can be operative to various extents for individual carbons in different molecules. However, only the first two are commonly observed.

Detailed mathematical and conceptual descriptions of ^{13}C relaxation mechanisms are provided elsewhere.[4-6]

Dipole–Dipole (DD) Relaxation. Dipole–dipole interactions between ^{13}C nuclei and neighboring magnetic nuclei (or unpaired electrons) can result in relaxation of the ^{13}C nuclei. The strength of the interaction depends on the square of the magnetogyric ratios (γ^2) and on the inverse sixth power of the distance between the interacting dipoles.

The dependence on the magnetic moment favors strong interactions with protons or with unpaired electrons if they are present in the sample. The sixth power distance dependence all but eliminates relaxation from non-nearest-neighboring protons. Relaxation of ^{13}C nuclei with one or more directly bonded protons (*protonated carbons*) is efficient because of the short internuclear distance, 1.09 Å.

The equation describing dipole–dipole relaxation for a C–H carbon in an isotropic, rigid tumbler introduces another important concept, eq 1, where R_1 is

$$\frac{1}{T_1^{DD}} = R_1^{DD} = \hbar^2\gamma_C^2\gamma_H^2 r^{-6}\tau_C \qquad (1)$$

the relaxation rate, $\hbar$ is Planck's constant divided by 2π, γ_C and γ_H are the magnetogyric ratios for ^{13}C and ^1H nuclei, r is the C–H internuclear distance, and τ_C is the molecular correlation time. Equation 1 is valid only in the "extreme narrowing" limit, where τ_C is very short relative to the reciprocal of the resonance frequency (in radians sec^{-1}). This condition holds for most organic compounds in nonviscous solutions. However, biopolymers and highly restricted synthetic polymer structures often violate the extreme narrowing condition.

The molecular correlation time, τ_C, approximates the time required for rotation of the molecule through 1 radian. Of course molecular motion in solution is not purely rotational, nor do molecules generally tumble as isotropic rigid bodies. The motional components described by τ_C do have real effects on T_1 processes. Rotational motions at rates close to the ^{13}C resonance frequency ($\sim 10^9$ radians sec^{-1} on 14 and 23 kG spectrometers) are most effective for DD relaxation. Motions significantly faster or slower than the Larmor frequency are not as effective. For organic molecules in solution τ_C is typically 10^{-11} to 10^{-13} sec depending on molecular size and symmetry, viscosity, temperature, etc. *For these molecules*

(4) (a) W. T. Huntress, Jr., *J. Chem. Phys.*, **48**, 3524 (1968); (b) D. E. Woessner, *ibid.*, **36**, 1 (1962); (c) *ibid.*, **42**, 1855 (1965); (d) A. Allerhand, D. Doddrell, and R. Komoroski, *ibid.*, **55**, 189 (1971); (e) D. Doddrell, V. Glushko, and A. Allerhand, *ibid.*, **56**, 3683 (1972).

(5) A comprehensive review of carbon-13 relaxation has been published: J. R. Lyerla, Jr., and D. M. Grant, *Int. Rev. Sci., Phys. Chem. Ser.*, **1**, 1 (1972).

(6) G. C. Levy, J. D. Cargioli, and F. A. L. Anet, *J. Amer. Chem. Soc.*, 95, 1527 (1973), and earlier papers.

increased molecular motion (shortening τ_C) lowers the efficiency of DD interactions and lengthens T_1^{DD}. Under these circumstances, increases in temperature and decreases in solution viscosity result in longer experimental relaxation times (when DD relaxation is operating).

The usefulness of ^{13}C T_1 measurements largely derives from relationships between molecular motions and relaxation. Equations describing these relationships for specific types of anisotropic tumbling and internal motions are available.[4] *In many cases it is not necessary to use any mathematics beyond arithmetic* in order to obtain *significant* information about molecular motion and structure.

Spin Rotation (SR) Relaxation. Small molecules and freely rotating CH_3 groups can be effectively relaxed by a mechanism involving local magnetic fields produced by the rotational motions of the molecule or group itself. In these cases SR relaxation often competes with DD relaxation for protonated carbons, while the SR interaction dominates the relaxation of nonprotonated carbons. At high temperatures and low viscosities T_1^{SR} becomes shorter as a result of increased molecular motion (larger populations in the higher rotational energy states). Observed SR relaxation times in small molecules are typically 15–50 sec.[2,5]

Chemical Shift Anisotropy (CSA) Relaxation. Significant anisotropy (directionality) in the shielding of a nucleus can give rise to fluctuating magnetic fields when the molecule tumbles in solution (relative to the fixed laboratory magnetic field). CSA relaxation is almost never significant for ^{13}C nuclei at normal spectrometer fields. Since the efficiency of CSA relaxation follows the square of the magnetic field, this mechanism may play a more important role in experiments performed at very high fields. However, even at 59 kG (63 MHz), CSA relaxation does not dominate relaxation for the nonprotonated carbon in toluene.[6]

Scalar (SC) Relaxation. A ^{13}C nucleus that is spin–spin (scalar) coupled to a quadrupolar nucleus X that is undergoing rapid spin–lattice relaxation may, in principle, be relaxed by the rapid modulation of the spin–spin coupling constant J_{C-X}. Scalar ^{13}C spin–lattice relaxation is very rare and has been observed thus far only for carbons attached to bromines.[6,7] Spin–spin SC relaxation is more common, since the requirements are less stringent.[1b]

Differentiation of Relaxation Mechanisms

There are several methods available for differentiation between the various relaxation mechanisms.[2,5,6] ^{13}C–^1H DD relaxation can be evaluated directly because it is the only mechanism that gives positive nuclear Overhauser enhancements (NOE's) in ^{13}C experiments using ^1H decoupling (denoted $^{13}C\{^1H\}$). The NOE is a by-product of the strong perturbation of the ^1H energy level populations as a result of decoupling.

In $^{13}C\{^1H\}$ experiments when ^{13}C–^1H DD relaxation is operative, partial or full equalization of the proton energy level populations results in establishment of an excess population of ^{13}C spins in the lower energy level. This increases the observed signals in $^{13}C\{^1H\}$ experiments. When the ^{13}C–^1H DD mechanism completely dominates ^{13}C relaxation the integrated peak areas will be three times larger in the $^{13}C\{^1H\}$ experiments.[8] The threefold enhancement $(1 + \eta)$ thus corresponds to 200% NOE or $\eta = 2.0$ (The theoretical maximum $^{13}C\{^1H\}$ NOE, η, is actually 1.988[8]). For ^{13}C nuclei where DD relaxation competes with other relaxation mechanisms, the contribution of the DD mechanism may be calculated if the experimental NOE is determined: (eq 2 and 3, where T_1^{obsd} is the observed T_1 and T_1^{DD} is the T_1 due to ^{13}C–^1H DD interactions).

$$\% \text{ DD relaxation} = \frac{\eta}{1.988} \times 100 \tag{2}$$

and

$$T_1^{DD} = T_1^{obsd} \frac{1.988}{\eta} \tag{3}$$

The SR mechanism may be distinguished from the DD relaxation both by reduction in observed NOE's and by its opposite dependence on temperature and viscosity.

The CSA mechanism is differentiated by its field dependence, mentioned above. Scalar relaxation may also exhibit a field dependence, although not in a simple way.

The contributions of different mechanisms to a carbon's relaxation may be calculated in some cases. These contributions add as relaxation rates. In eq 4a and 4b the other relaxation terms refer to contributions such as dipolar relaxation from dissolved oxygen or paramagnetic additives.

$$R_1^{obsd} = R_1^{DD} + R_1^{SR} + R_1^{CSA} + R_1^{SC} + R_1^{other} \tag{4a}$$

$$\frac{1}{T_1^{obsd}} = \frac{1}{T_1^{DD}} + \frac{1}{T_1^{SR}} + \frac{1}{T_1^{CSA}} + \frac{1}{T_1^{SC}} + \frac{1}{T_1^{other}} \tag{4b}$$

The ^{13}C T_1 behavior of many large molecules is characterized by isotropic overall molecular motion and by the predominance of ^{13}C–^1H DD relaxation, even for nonprotonated carbons.[4d] Carbon T_1's in these molecules are very short. Protonated carbons can have T_1's shorter than 100 msec, while nonprotonated carbon T_1's typically range from 1 to 5 sec. With T_1's shorter than *ca.* 0.5 sec (this number depends on magnetic field homogeneity, wide-band proton decoupling power, and the time used for acquisition of each FID) spectral line broadening becomes evident. In native biopolymers some carbon T_1's may be extremely short, *e.g.*, 10 msec. These carbons will have spectral line widths defined by $1/\pi T_1$ (about 30 Hz).

In smaller, more symmetrical, molecules, tumbling is more rapid and other mechanisms may compete with relatively inefficient ^{13}C–^1H DD relaxation. Observed T_1's for protonated carbons may exceed 10–20

(7) (a) R. Freeman and H. Hill, "Molecular Spectroscopy 1971," Institute of Petroleum, London, 1971; (b) T. C. Farrar, S. J. Druck, R. R. Shoup, and E. D. Becker, *J. Amer. Chem. Soc.*, **94**, 699 (1972); (c) G. C. Levy, *J. Chem. Soc., Chem. Commun.*, 352 (1972); (d) J. R. Lyerla, Jr., D. M. Grant, and R. D. Bertrand, *J. Phys. Chem.*, **75**, 3967 (1971).

(8) K. F. Kuhlman and D. M. Grant, *J. Amer. Chem. Soc.*, **90**, 7355 (1968).

Table I
^{13}C Relaxation in Benzene and Toluene[a]

	Carbon	T_1	NOE (η)	T_1^{DD}	T_1^{SR}	T_1^{O2}	T_1^{CSA}
Benzene							
Degassed	All	29.3	1.60	37	146		
Undegassed	All	23.0	1.30	35		107	
Toluene							
Degassed	1	89	0.59	297	130		$\gtrsim 3000^c$
	2,3,4[b]	22	1.68	26	147		$\gtrsim 3000^c$
Undegassed	1	58	0.43	270		155	
	2,3,4[b]	19.5	1.45	27		135	
	7 (CH_3)	16.3	0.61	53	28		

[a] From ref 6 and G. C. Levy, *J. Chem. Soc., Chem. Commun.*, 47 (1972). Measurements at 25.2 MHz and 38°. All T_1's in seconds. Errors in calculated T_1 contributions may exceed 25%. Experimental T_1's ±5–10%. [b] Average values for C-2, C-3, and C-4. [c] Estimated from calculations and experiments at 63 MHz.[6]

sec, while nonprotonated carbons can have T_1's > 100 sec. To obtain useful T_1 results with these smaller molecules, samples must be degassed to prevent atmospheric oxygen from contributing to ^{13}C relaxation. Table I summarizes observed T_1 and NOE data for benzene and toluene.

The contributions of individual relaxation mechanisms given in Table I were calculated from the experimental T_1 and NOE data shown and from 63-MHz T_1 data obtained with a superconducting solenoid spectrometer (to estimate T_1^{CSA}). It is important to realize that the individual T_1^{xx} terms are not extremely accurate; small errors propagate through the calculations.

Some interesting trends may be noted. In degassed samples, the nonprotonated carbon of toluene is primarily relaxed by the SR interaction. T_1^{SR} for the other ring carbons in toluene and for the ring carbons of benzene is comparable to T_1^{SR} for C-1. The significance of SR relaxation changes, of course, depending on the efficiency of competing mechanisms. The CH_3 carbon of toluene has a very short T_1^{SR} due to rapid internal spinning of the methyl top.

The remainder of this article discusses methods and applications of ^{13}C relaxation studies. For the most part these applications will concern carbons undergoing predominantly ^{13}C–^1H DD relaxation, since the greatest number of organic compounds fall in this class.

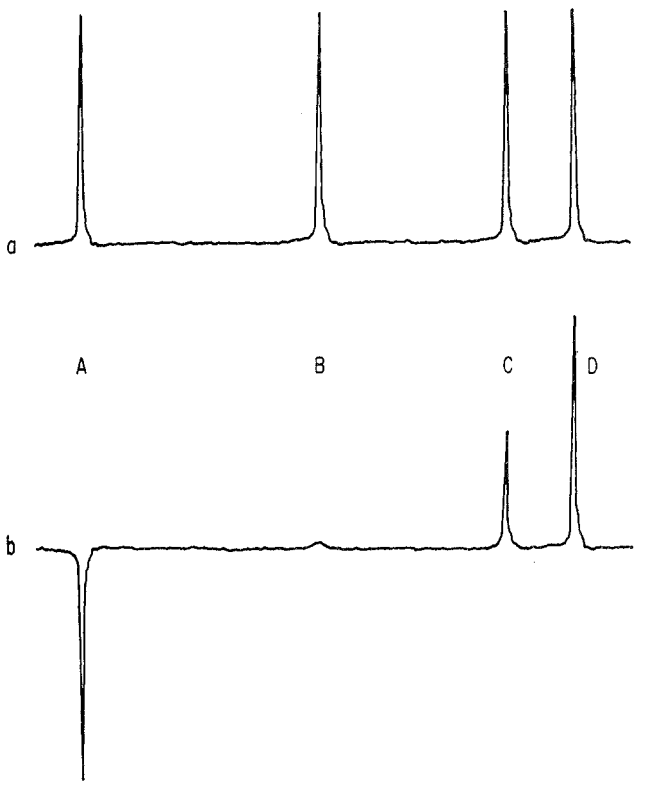

Figure 2. Simulated (a) normal FT and (b) inversion-recovery Fourier transform (IRFT) ^{13}C nmr spectrum.[2] Four cases (A → D) are indicated in part b: (A) $t \ll T_1$; (B) $t \sim T_1 \ln 2$; (C) $t \sim T_1$; (D) $t \gg T_1$.

Experimental Measurement of T_1

Various experiments have been designed to measure spin-lattice relaxation times using both swept continuous wave (cw) nmr[9] and pulse excitation.[4d,e,6,10] For versatile ^{13}C T_1 studies at natural abundance one of the several pulse Fourier transform methods must be used. All these experimental methods share a single characteristic: they all monitor the z magnetization as a function of time, following a perturbation of the initial $M = M_0$ case (see Figure 1). One of the common pulse sequences for T_1 measurements, the *inversion-recovery sequence,* first inverts M with an isolated 180° pulse, then follows after a time t with a 90° pulse to monitor the relaxation from $-M_0$ back toward $+M_0$. The 90° pulse results in a FID. Fourier transformation of the FID gives a partially relaxed spectrum in which the intensity of each resonance line is proportional to the z magnetization at the time of the 90° pulse and t sec after the 180° pulse. Spectral lines will vary in intensity and may be inverted or in phase, or may be nulled, depending on the relationship between t and T_1. Four examples are given in Figure 2b. Accurate T_1's can be calculated from semi-log plots of peak intensity as a function of t. For ^{13}C nmr studies a single (180°–t–90°) pulse sequence will not usually give sufficient signal strength, and time averaging is required. The pulse sequence then used is $(-T-180°-t-90°-)_x$, where T is a long waiting period to ensure complete relaxation between individual (180°–t–90°) sequences (in practice, T must be 3–4

(9) Examples: (a) K. F. Kuhlman, D. M. Grant, and R. K. Harris, *J. Chem. Phys.*, **52**, 3439 (1970); (b) A. Olivson, E. Lippmaa, and J. Past, *Eesti NSV Tead. Akad. Toim. Fuus., Mat.*, **16**, 390 (1967).

(10) Examples: (a) R. Freeman and H. D. W. Hill, *J. Chem. Phys.*, **53**, 4103 (1970); (b) *ibid.*, **54**, 3367 (1971); (c) D. E. Jones, *J. Magn. Resonance*, **6**, 191 (1972).

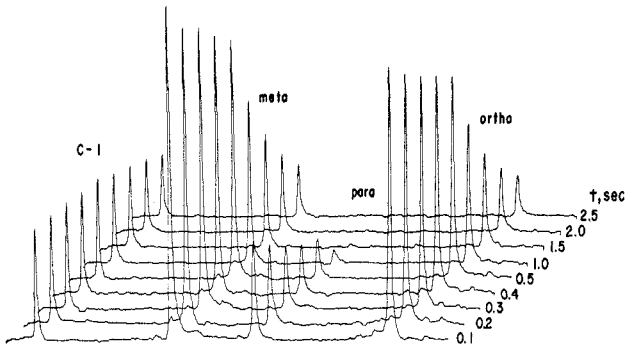

Figure 3. Set of IRFT spectra for anilinium acetate in acetic acid. T_1 for the nonprotonated carbon C-1 cannot be determined from these data because T is too short (7 sec).

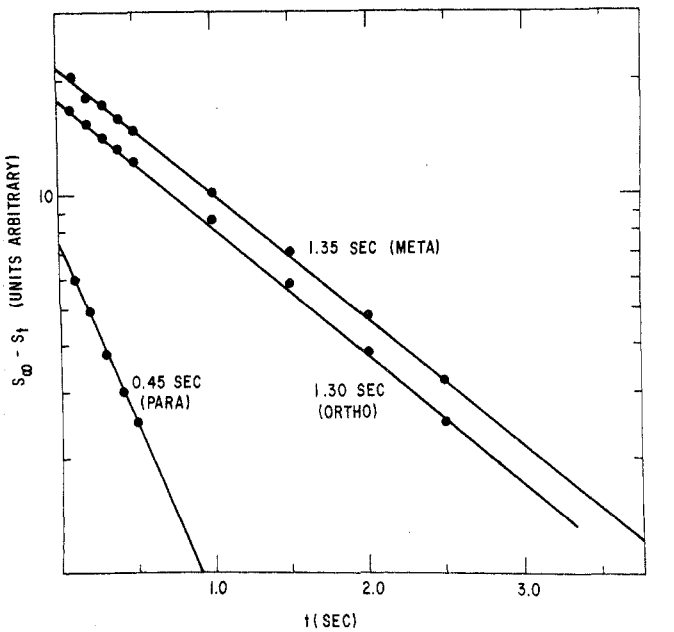

Figure 4. Semi-log plot of the data from Figure 3. The para carbon T_1 is much shorter than T_1 for the ortho and meta carbons. This results from highly anisotropic molecular tumbling in solution; the ionic site is locked into the solvent matrix (see ref 6 and arguments below).

times the longest T_1 to be determined). The sequence may be repeated many times for each value of t, but with concentrated samples $x < 100$. The procedure is time consuming in any event, largely because of the waiting period T which can be several hundred seconds where T_1's are long (for example, nonprotonated carbons in some small, symmetrical molecules). Fortunately, computer control often allows these experiments to be performed overnight, without operator assistance.

A variation of the inversion-recovery pulse sequence developed by Freeman and Hill[10b] results in spectral data representations with all signals in the same sense. This pulse sequence is $(-T\text{-}90°_\infty\text{-}T\text{-}180°\text{-}t\text{-}90°_t\text{-})_x$, where T and t have the usual characteristics and $90°_\infty$ represents an "isolated" 90° pulse that follows the long waiting period.

Long-term drifts in the spectral resolution and/or spectrometer gain are partly cancelled using this pulse sequence, as a result of alternating addition and subtraction operations. The second half of this scheme is the standard (180°-t-90°) sequence. The computer alternately adds the FID data from the $90°_\infty$ pulses and subtracts the FID's resulting from the $90°_t$ pulses. These spectra then plot $(S_\infty - S_t)$, where S_∞ *and* S_t are the signals obtained after Fourier transformation of the FID's from the $90°_\infty$ and the $90°_t$ pulses, respectively. Figures 3 and 4 show a spectral set and T_1 data plot obtained with this pulse sequence.

Another scheme for measuring ^{13}C T_1's is the method of *progressive saturation*.[11] Here the sample is subjected to a train of equispaced 90° pulses. Nuclei with T_1's that are long relative to the pulse interval are largely saturated and yield, after Fourier transformation, lines of greatly reduced intensity. Variation of the pulse interval t and plotting of the data as described above can give results comparable in accuracy with those obtained from the inversion-recovery pulse sequences. The advantage of this method is the omission of long waiting time T between repetitions of the sequence. Twofold experimental time savings may be achieved for carbons with long T_1's, but it is necessary to carefully adjust pulse widths to 90° and to use a homospoil pulse (or equivalent) to cancel residual x-y magnetization after each FID acquisition.

(11) R. Freeman, H. D. W. Hill, and R. Kaptein, *J. Magn. Resonance*, 7, 82 (1972), and earlier papers.

Professor N. Boden[12] has suggested that IRFT and PSFT be used to designate, respectively, inversion-recovery and progressive saturation FT relaxation experiments while PRFT would be used to indicate partially relaxed (*or*, partially recovered) FT experiments without distinguishing between the methods.

The IRFT and PSFT methods are both capable of yielding results to 1-2% precision, assuming high spectral signal-to-noise ratios, and maximum control of experimental variables. Typical ^{13}C T_1 studies are accurate and reproducible to 5-15%. Chemical information can often be obtained from semiquantitative T_1's (±30-50%).

Applications

Carbon-13 spin-lattice relaxation measurements have many applications to problems in organic chemistry. Most of the applications rely on the relationships between the ^{13}C T_1's and overall and internal molecular motions. These motions are functions of molecular size, symmetry, and stereochemistry, as well as elemental composition and electronic and chemical bonding effects.

Carbon-13 spin-spin relaxation times can also be measured, although those experiments are much more difficult than measurements of T_1.[13] With some exceptions (*e.g.*, chemical exchange situations) little additional information is derivable from the more difficult T_2 measurements. This Account will deal solely with T_1 studies.

Determination of Organic Molecular Structure. Several types of information derived from ^{13}C T_1 measurements can be used for determination or con-

(12) N. Boden, *Nucl. Magn. Resonance*, 1, 141 (1972).

(13) R. Freeman and H. D. W. Hill, *J. Chem. Phys.*, **55**, 1985 (1971); R. R. Shoup and D. L. Vanderhart, *J. Amer. Chem. Soc.*, **93**, 2053 (1971); U. Haeberlen, H. W. Spiess, and D. Schweitzer, *J. Magn. Resonance*, 6, 39 (1972).

firmation of organic structure. For example, T_1 experiments distinguish between protonated and nonprotonated carbons based on the differences in C–H internuclear distances. The ^{13}C T_1 values for mescaline (I) even distinguish between the three types of

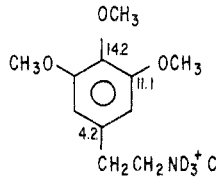

mescaline - d_3 (I) [T_1's in sec]

nonprotonated carbons based on the C–H distances to nearby (ortho) protons. The relaxation of this intermediate-sized, polar molecule is dominated by the ^{13}C–^{1}H DD mechanism. C-4, with no ortho protons, has the longest T_1 (14.2 sec). T_1 for C-3 and C-5 (each with one ortho proton) is somewhat shorter, while the relaxation of C-1 is fastest due to the two ortho protons and the CH_2 protons.[14]

In many cases it is also possible to differentiate between CH, CH_2, and CH_3 carbons. Allerhand has shown that medium-sized or large relatively rigid organic molecules (*e.g.*, steroid skeletons) often tumble more-or-less isotropically in solution.[4d] Under these circumstances, the ^{13}C T_1's for CH and CH_2 carbons would be in a ratio of 2:1. The two types of carbons are subject to the same motion, but the CH_2 carbon is relaxed by *two* protons; thus its relaxation is twice as efficient. In principle, CH_3 carbon T_1's in these molecules could be three times shorter than CH T_1's. However, rapid internal rotation (see below) of the CH_3 groups results in longer T_1's than predicted based on the number of attached protons. In molecules where the CH_3 group is sterically restricted and its independent rotation is slow relative to overall molecular tumbling, the CH_3 T_1 approaches $\frac{1}{3}T_1$ for CH carbons in the molecule.

Differentiation of nonprotonated, CH, CH_2, and CH_3 carbons can be achieved by other means in many compounds, in particular, by off-resonance ^{1}H decoupling, but the decoupling method becomes increasingly impractical with increasing spectral complexity. Allerhand has used ^{13}C T_1's to differentiate carbons in very complex molecules[15] where decoupling methods would be very difficult.

Anisotropic Tumbling and Internal Rotation. Many small compounds tumble anisotropically in solution. Preferential tumbling modes occur, resulting from inertial, frictional, and electrostatic effects, as well as from intramolecular and intermolecular interactions. Anisotropic molecular tumbling may also occur with large molecules, although localized electrostatic and inertial effects tend to cancel out in these systems.[16] For large polycyclic molecules, the central molecular framework may orient isotropically while peripheral molecular fragments have shorter effective correlation times, τ_c^{eff}, resulting from internal motions that are comparable with, or faster than, overall molecular reorientation. The angular CH_3 groups and 17-alkyl chains of steroids exhibit this kind of behavior.[4d]

Table II
Anisotropic Tumbling in Monosubstituted Benzenes[a]

Substituent	$T_1^{o,m}/T_1^{p}$ [b]	Approximate tumbling ratio
CH_3	1.3	2
$C(CH_3)_3$	1.8	3.5
C≡CH	1.7	3.2
Ph	1.8	3.5
C≡CPh	2.4	7
C≡CC≡CPh	4.9	17
NO_2	1.4	2.2
OH	1.5	2.5

[a] Data from ref 6 and 17. [b] T_1 for the ortho and meta carbons ÷ $2T_1$ for the para carbon.

The effect of anisotropic overall or internal motion on T_1's for the different carbons in a molecule depends on the angular relationships between each carbon and the proton(s) relaxing it *relative to the preferred mode of rotation.* For example, in monosubstituted benzenes rotation around the C_2 molecular symmetry axis (coincident with the substituent–ring bond) is favored.[6] If the substituent is large and heavy or highly polar, then rotation around the C_2 axis may be 5–20 times faster than rotation around the two remaining perpendicular axes. Rotation

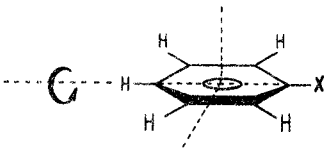

around the C_2 symmetry axis does not lead to any modulation in the dipole–dipole interaction of the para ^{13}C and its directly attached proton. This motion does not shorten τ_c^{eff} for the para carbon. However, such a rotation does lead to relaxation for the ortho and meta carbons because the C–H bonds in these instances make angles (θ) of 60 and 120° with the C_2 axis. In the limit of very much faster rotation about the long C_2 axis than about the shorter axes of these molecules, T_1 for the ortho and meta carbons should be increased by a factor of $[\frac{1}{2}(3\cos^2\theta - 1)]^{-2}$ (*i.e.*, 64 for θ = 60°, 120°) over T_1 for the para carbon.[4d,6] Below the limit of anisotropic motion, calculations can predict approximate motional anisotropy from observed T_1 values.[4d,6] Table II lists some monosubstituted benzenes with estimates of their anisotropic motion.

The motional behavior of substituted benzenes can be used to facilitate resonance assignments, as in the ^{13}C FT spectrum of 3-bromobiphenyl, shown in Figure 5. The ^{13}C T_1's indicated next to each protonated carbon resonance allow differentiation between the closely spaced lines. C-4 and C-4′ have the short-

(14) Intermolecular ^{13}C–^{1}H DD relaxation to protonated and nonprotonated carbons can usually be neglected.[6]

(15) D. Doddrell and A. Allerhand, *Proc. Nat. Acad. Sci. U. S.*, 68, 1083 (1971).

(16) In synthetic and biopolymers certain molecular motions will be highly restricted.

(17) G. C. Levy, D. M. White, and F. A. L. Anet, *J. Magn. Resonance*, 6, 453 (1972).

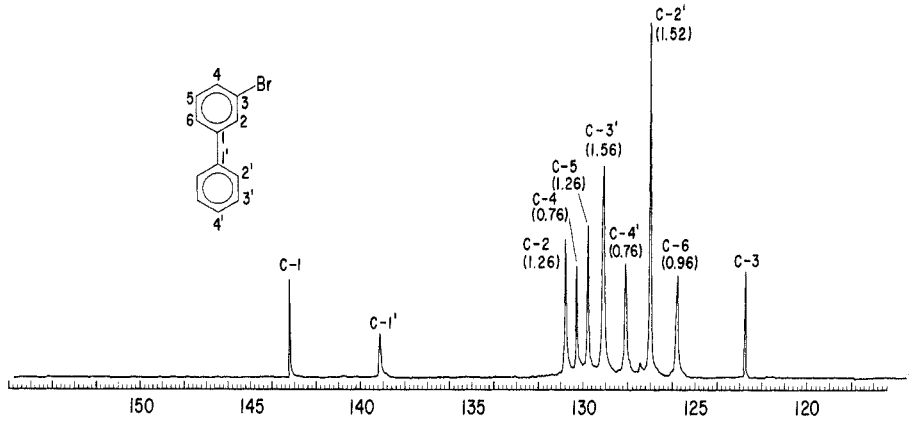

Figure 5. ^{13}C FT spectrum of 3-bromobiphenyl. ^{13}C T_1's for protonated (C–H) peaks in seconds (±5%). ^{13}C chemical shifts (ppm) relative to Me_4Si.

est T_1's since they are para to large phenyl rings. C-6 has a short T_1 because it is para to the bromine substituent. The T_1's for C-2′ and C-3′ are longer than for C-2 and C-5, indicating that some internal spinning of the nonbrominated phenyl ring occurs (in monosubstituted benzenes it is not usually possible to distinguish between "internal" phenyl spinning around the C–X bond and rapid overall rotation around the C_2 molecular axis).

Anisotropic overall and internal motions of groups other than phenyl rings give rise to qualitatively similar behavior. The effect on protonated carbon T_1's depends on the specific geometry involved. In the limit of rapid internal spinning of a CH_3 carbon, T_1^{CH3} will be three times T_1 for a C–H carbon in the same molecule, or nine times T_1^{CH3} for a CH_3 carbon which is not spinning. In organometallic sandwich compounds the two rings may spin independently,[18] resulting in different T_1's for the protonated carbons of the two rings. The angle θ between the C–H vectors and the internal motion in this case is 90°, and the effect is not as pronounced as in substituted benzenes. Very rapid internal spinning of one ring relative to another results in a T_1 ratio of only four. T_1 ratios of 2 and 2.4 have been observed in two monosubstituted ferrocenes.[18] These correspond to ratios of *ca.* 4 and 7 for the spinning of the unsubstituted *vs.* substituted rings.

Segmental Motion. Localized motion along an aliphatic chain (or along another molecular substructure) is called segmental motion. Segmental motion has been monitored in long alkyl chains by ^{13}C T_1 measurements on 1-decanol[19] and lecithin models for biological membranes.[20] Segmental motion has been observed along shorter chains in some aliphatic amides and oximes,[21] and for the alkyl side chain in cholesteryl chloride.[4d] To observe segmental motion from ^{13}C T_1 measurements the local motion must approximate or exceed the overall tumbling rate of the molecule. The multiple degrees of freedom inherent in these segmental motions preclude exact representation by formulae. However, it is possible to represent the internal motions by calculating approximate effective correlation times. Thus τ_c^{eff} for C-1 of decanol is seven times longer than τ_c^{eff} for C-10. Intermolecular hydrogen bonding restricts motion at the hydroxylic end of the molecule. In lecithins, the large molecular fragment formed by the linking of three alkyl chains together restricts motion near the junction of the chains. For sonicated dipalmitoyllecithin vesicles (bilayer structures) τ_c^{eff} decreases by a factor of almost 50 along the 15 carbon aliphatic chains.[20a]

Chart I[a]

$CH_3—CH_2—CH_2—CH_2—R$

3.1	2.3	1.6	1.1	*N,N*-di-*n*-butylformamide
3.1	2.2	1.6	1.1	1-decanol
3.3	1.8	1.1	(*)[a]	dipalmitoyllecithin

[a] Unresolved from other central carbons.[20a]

Segmental motion along short chains is less marked. Intermolecular hydrogen bonding does not slow overall molecular reorientation enough in 1-butanol to observe greatly different ^{13}C T_1's for the four carbons.[21] However, in *N,N*-di-*n*-butylformamide the molecular anchor represented by the Y junction at nitrogen does restrict motion sufficiently to observe segmental motion along the four carbon chains. In this case the ^{13}C T_1's are quite similar to the T_1's observed for the last four carbons of the alkyl chains in decanol and dipalmitoyllecithin (Chart I).

The constancy of the T_1's for the free ends of these very different alkyl chains implies a "*limiting microviscosity*" effect. For the free ends of these alkyl chains the microviscosity bears no relation to macroscopic viscosity, or to the rate of overall molecular reorientation!

Intermolecular hydrogen bonding interactions were insufficient to effectively anchor the CH_2OH group for the short-chain alcohol butanol. By contrast, examination of the *n*-butylammonium ion in various media indicates that ionic sites may be more effectively anchored in some solvent matrices.[22] Table III

(18) G. C. Levy, *Tetrahedron Lett.*, 3709 (1972).
(19) D. Doddrell and A. Allerhand, *J. Amer. Chem. Soc.*, **93**, 1558 (1971).
(20) (a) Y. K. Levine, N. J. M. Birdsall, A. G. Lee, and J. C. Metcalfe, *Biochemistry*, **11**, 1416 (1972); (b) J. C. Metcalfe, *et al.*, *Nature (London)*, **233**, 201 (1971).
(21) G. C. Levy and G. L. Nelson, *J. Amer. Chem. Soc.*, **94**, 4897 (1972).
(22) (a) G. C. Levy, *J. Chem. Soc., Chem. Commun.*, 768 (1972); (b) G. C. Levy, J. D. Cargioli, and J. A. Halstead, unpublished results.

Table III
^{13}C Relaxation Behavior of n-$BuNH_2$ and n-$BuNH_3^+CF_3CO_2^-$

	Solution	Concn (w/w)	T_1, sec C-1	C-2	C-3	C-4
n-$BuNH_2$	Neat		13.4	13.4	15.0	12.1
n-$BuNH_3^+$	Dioxane	20	0.88	1.54	1.95	3.35
$CF_3CO_2^-$	CH_2Cl_2–acetone	24	0.91	1.67	2.41	3.90
	CF_3CO_2H	15.4	1.54	2.30	3.12	3.98
		28.2	0.97	1.50	2.13	3.46
	CD_3OD	20	3.10	4.52	5.35	6.00
	D_2O	20	3.75	4.26	5.00	5.00

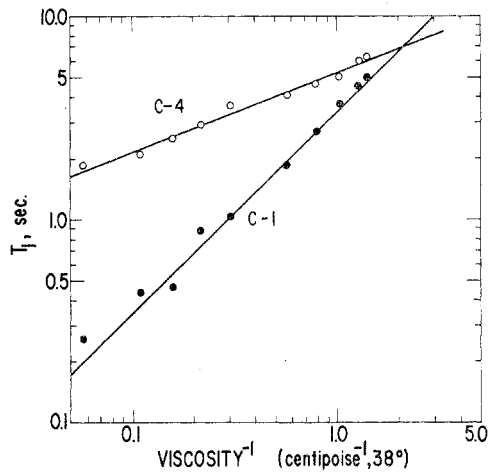

Figure 6. Log-log plot of ^{13}C T_1's *vs. viscosity*$^{-1}$, n-$BuNH_3^+CF_3CO_2^-$ in D_2O. All measurements, 38°. T_1's determined at 25 MHz; accuracy varies depending on concentration, from ±5 to 20%.

lists ^{13}C T_1's for neat n-$BuNH_2$ and n-$BuNH_3^+$-CF_3CO^- in several solvent systems.

The relaxation times of the parent amine indicate overall tumbling is more rapid than in n-BuOH (T_1's = 3–4 sec) and a small degree of segmental motion. By contrast, the overall motion of the ion in nonpolar solvents is greatly reduced (note the > tenfold reduction in T_1 for C-1) with a pronounced degree of observed segmental motion. In polar media (*e.g.*, CD_3OD, D_2O) the ion is presumably more easily stabilized electrostatically, making solvent and counterion moieties less interactive. In these media overall motion increases and segmental motion is less pronounced. The macroviscosities of these solutions were not related to the observed T_1 behavior.[23] In fact, the CH_2Cl_2–acetone solution had the lowest viscosity. The ion was examined in D_2O solutions over the concentration range 5–95 wt % (corresponding to >200:1 and ~1:2 mol ratios of D_2O:ion respectively).[22b] Through this range of concentrations the solution viscosity and polarity undergo extreme changes. Figure 6 shows the T_1 data for C-1 and C-4 plotted (log–log) against the inverse viscosity. The data for C-1 form the anticipated straight line with slope = 1 indicative of a monotonic dependence. The data for C-4 also form a straight-line dependence, but the slope is only 0.3. The linear correlation of T_1 for C-4 with (viscosity)$^{-1}$ may be coincidental, but the reduced dependence on viscosity is a real result of segmental motion.

Intramolecular Steric Effects. ^{13}C relaxation times may be used to examine intramolecular steric interactions. Calculations of energy barriers for rotation around single bonds are sometimes possible,[24] but it is generally difficult to relate T_1 data to specific steric interactions. The T_1 data usually relate to the presence of conformational energy wells. A sterically compressed group may still undergo rapid reorientation if unfavorable interactions are comparable for all rotomeric conformers. Comparison of the CH_3 and ring carbon T_1 data for 1-methylnaphthalene (II) and 9-methylanthracene (III) is illustrative. In II the

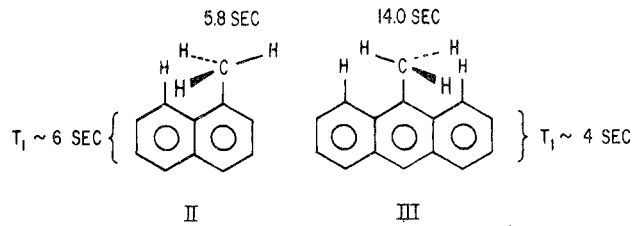

peri proton prevents rapid rotation of the CH_3 group. The most stable rotomer (shown) is at the bottom of a relatively deep energy well. Compound III has two sterically unfavorable peri proton interactions, but the CH_3 group spins rapidly because no rotomeric conformer has significantly lower energy.

In methyl ethyl ketoxime somewhat analogous behavior is observed.[21] The CH_3 carbon syn to the N–OH groups in the predominant isomer IVa spins faster than the CH_3 carbon in isomer IVb. Presum-

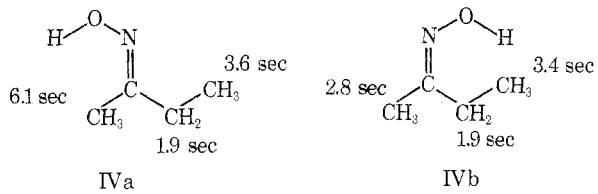

ably, opposing steric interactions between the IVa CH_3 protons and the NOH and CH_2 groups are similar in magnitude. In isomer IVb the CH_3 group may adopt a relatively fixed conformation.

Phenyl benzoate (V) in dimethyl-d_6 sulfoxide at

(23) The viscosity and T_1 data were consistent for the two CF_3CO_2H solutions, however.

(24) T. D. Alger, D. M. Grant, and R. K. Harris, *J. Phys. Chem.*, **76**, 281 (1972).

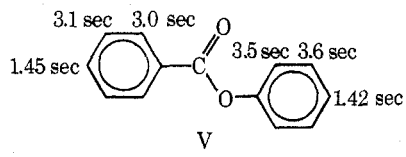

V

68° shows the following T_1's. The $T_1^{o,m}/T_1^{p}$ ratio is distinctly greater for the phenoxy ring than for the benzoyl group, presumable reflecting a lower barrier to rotation about the phenyl–oxygen bond than about the phenyl–carbonyl bond.

Other Applications. Some of the most important future applications for ^{13}C relaxation studies involve characterization of proteins, nucleic acids, and other biopolymer molecules.[25] Structure analysis of synthetic high polymers in solution from ^{13}C T_1 (and line shape T_2) measurements is also very promising.[26] Studies of solution effects such as hydrogen bonding and ion pairing may give new insight into these processes.[6,22,27,28] The ^{13}C T_1 experiment shown in Figures 3 and 4 illustrates the effects of strong solvation of ions. The tumbling of nonprotonated aniline is nearly isotropic, whereas the anilinium ion rotates approximately ten times faster around the C_2 axis. Other ^{13}C relaxation studies of rapid molecular motions will undoubtedly emerge soon, showing additional applications for this important new technique.

I wish to acknowledge the valuable contributions of Professor F. A. L. Anet and Joseph D. Cargioli. Professors D. M. Grant, A. Allerhand, and J. B. Grutzner and Doctors R. Freeman, H. M. Relles, and E. D. Becker provided helpful discussions. I also thank the management of General Electric Corporate Research and Development for their support.

(25) Recent references include: R. A. Komoroski and A. Allerhand, *Proc. Nat. Acad. Sci. U. S.*, **69**, 1804 (1972); V. Glushko, P. J. Lawson, and F. R. N. Gurd, *J. Biol. Chem.*, **247**, 3176 (1972); A. M. Nigen, P. Keim, R. C. Marshall, J. S. Morrow, and F. R. N. Gurd, *ibid.*, **247**, 4100 (1972).

(26) J. Schaefer and D. F. S. Natusch, *Macromolecules*, **5**, 416 (1972); J. Schaefer, *ibid.*, **5**, 427 (1972).

(27) G. C. Levy, *J. Magn. Resonance*, 8, 122 (1972).

(28) G. C. Levy and J. D. Cargioli, *J. Magn. Resonance*, in press.

The S-Peptide–S-Protein System: a Model for Hormone–Receptor Interaction[1a]

Frances M. Finn and Klaus Hofmann*

Protein Research Laboratory, University of Pittsburgh, School of Medicine, Pittsburgh, Pennsylvania 15261

Received October 17, 1972

Structure–function studies with peptide hormones have provided considerable understanding of the contribution of individual amino acid residues within a sequence to overall biological activity. As a result of these investigations, it is now recognized that large structural modifications can be tolerated in many cases without loss of physiological activity. An adrenocorticotropic hormone ($ACTH_{1-20}$-amide[1b]) one-half the size of natural ACTH is fully active as concerns steroidogenesis and ascorbic acid depletion.[2] Recently, still shorter analogs with 5–10 times the activity of the natural molecule have been produced.[3,4]

The C-terminal tetrapeptide amide of gastrin is another example of a hormone fragment possessing biological activity. The natural heptadecapeptide amide is about fivefold more potent than the fragment, but the tetrapeptide amide still possesses the full spectrum of biological actions.[5] Furthermore, a number of amino acid substitutions can be made in peptide hormone fragments without decreasing their potency.

On the basis of these and other similar findings it was possible to formulate some generalizations regarding the role of amino acid residues within these structures.[6] Two major functional classes of amino acids seem to exist: those concerned with binding the

Dr. Klaus Hofmann's primary research interests are the chemistry and biochemistry of biologically important natural products. He received his graduate training under L. Ruzicka at the ETH in Zürich, where he received his Ph.D. in 1936. After 2 more years in Zürich and 2 years at the Rockefeller Institute for Medical Research with the late Max Bergmann, he joined the group of Vincent du Vigneaud at Cornell Medical College to work on the isolation and structure proof of biotin. After a 2-year residence as a scientific guest at the Laboratories of Ciba Pharmaceutical Products, Inc., he moved to the University of Pittsburgh in 1944. He is now Professor of Experimental Medicine and Director of the Protein Research Laboratory, University of Pittsburgh School of Medicine.

Dr. Frances Finn received her Ph.D. from the University of Pittsburgh in 1964 with Professor Hofmann and remains as Assistant Research Professor of Biochemistry. In 1964–1965 she was a U. S. Public Health Postdoctoral Fellow, working with Professor Westheimer at Harvard.

(1) (a) Work from the Protein Research Laboratory was generously supported by the National Institutes of Health, Grant No. AM01128, and by the Hoffmann-La Roche Foundation. (b) Three letter abbreviations of amino acids are those suggested by IUPAC (*J. Biol. Chem.*, **241**, 2491 (1966)). Synthetic peptides are abbreviated according to the following scheme, *e.g.*, Orn^{10}-S-$peptide_{1-14}$ denotes an analog corresponding to positions 1–14 in the sequence of natural S-peptide but containing an ornithine residue instead of arginine in position 10. The notation 3-$CMHis^{12}$-S-$peptide_{1-14}$ refers to a tetradecapeptide containing a carboxymethyl group on nitrogen 3 of the aromatic ring of histidine-12. F-Orn = N^{ϵ}-formylornithine; Met(→O) = methionine *d*-sulfoxide. Amino acids are of the L configuration.

(2) K. Hofmann, H. Yajima, T-Y. Liu, N. Yanaihara, C. Yanaihara, and J. Humes, *J. Amer. Chem. Soc.*, **84**, 4481 (1962).

(3) B. Riniker and W. Rittel, *Helv. Chim. Acta*, **53**, 513 (1970).

(4) R. Geiger, *Justus Liebigs Ann. Chem.*, **750**, 165 (1971).

(5) H. J. Tracy and R. A. Gregory, *Nature (London)*, **204**, 935 (1964).

(6) K. Hofmann, *Brookhaven Symp. Biol.*, **13**, 184 (1960).